Inorg. Chem. **2003**, *42*, 2362–2367

Inorganic Chemistry

Article

Syntheses and Oxidation of Methyloxorhenium(V) Complexes with Tridentate Ligands

Xiaopeng Shan, Arkady Ellern, Ilia A. Guzei, and James H. Espenson*

Ames Laboratory and Department of Chemistry, Iowa State University, Ames, Iowa 50011

Received November 12, 2002

Four new methyloxorhenium(V) compounds were synthesized with these tridentate chelating ligands: 2-mercaptoethyl sulfide (abbreviated HSSSH), 2-mercaptoethyl ether (HSOSH), thioldiglycolic acid (HOSOH), and 2-(salicylideneamino)-benzoic acid (HONOH). Their reactions with $MeReO_3$ under suitable conditions led to these products: MeReO(SSS), **1**, MeReO(SOS), **2**, MeReO(OSO)(PAr_3), **3**, and MeReO(ONO)(PPh_3), **4**. These compounds were characterized spectroscopically and crystallographically. Compounds **1** and **2** have a five-coordinate distorted square pyramidal geometry about rhenium, whereas **3** and **4** are six-coordinate compounds with distorted octahedral structures. The kinetics of oxidation of **2** and **3** in chloroform with pyridine *N*-oxides follow different patterns. The oxidation of **2** shows first-order dependences on the concentrations of **2** and the ring-substituted pyridine *N*-oxide. The Hammett analysis of the rate constants gives a remarkably large and negative reaction constant, $\rho = -4.6$. The rate of oxidation of **3** does not depend on the concentration or the identity of the pyridine *N*-oxide, but it is directly proportional to the concentration of water, both an accidental and then a deliberate cosolvent. The mechanistic differences have been interpreted as reflecting the different steric demands of five- and six-coordinate rhenium compounds.

Introduction

The oxidation of rhenium(V) complexes to rhenium(VII)[1] is an essential step in the catalytic cycle by which such a pair catalyzes oxygen atom transfer reactions.[2−10] Steric demand is always an important issue for such catalysts.[11−13] Different ligands for rhenium(V) complexes have been employed, especially those with "3 + 1",[14−16] "3 + 2",[17,18] and "3 + 1 + 1"[19,20] coordination shells. They differ in geometry as well as coordination number.

In this paper, we describe the syntheses of four new rhenium(V) compounds with tridentate ligands, the molecular structures of which are displayed in Chart 1. The oxidation of three of these compounds was investigated. Compound **4** was not studied because of its insolubility.

Experimental Section

Materials and Instrumentation. Methyltrioxorhenium(VII), CH_3ReO_3 or MTO, was prepared from sodium perrhenate, tetramethyl tin, and chlorotrimethylsilane.[21] The di(benzenethiolato)-

---

* To whom correspondence should be addressed. E-mail: espenson@ameslab.gov.

(1) Lente, G.; Espenson, J. H. *Inorg. Chem.* **2000**, *39*, 4809−4814.
(2) Arias, J.; Newlands, C. R.; Abu-Omar, M. M. *Inorg. Chem.* **2001**, *40*, 2185−2192.
(3) Arterburn, J. B.; Nelson, S. L. *J. Org. Chem.* **1996**, *61*, 2260−2261.
(4) Arterburn, J. B.; Perry, M. C. *Org. Lett.* **1999**, *1*, 769−771.
(5) Gable, K. P.; Brown, E. C. *Organometallics* **2000**, *19*, 944−946.
(6) Gunaratne, H. Q. N.; McKervey, M. A.; Feutren, S.; Finlay, J.; Boyd, J. *Tetrahedron Lett.* **1998**, *39*, 5655−5658.
(7) Huang, R.; Espenson, J. H. *J. Mol. Catal. A* **2001**, *168*, 39−46.
(8) Wang, Y.; Espenson, J. H. *Org. Lett.* **2000**, *2*, 3525−3526.
(9) Wang, Y.; Espenson, J. H. *Inorg. Chem.* **2002**, *41*, 2266−2274.
(10) Wang, Y.; Lente, G.; Espenson, J. H. *Inorg. Chem.* **2002**, *41*, 1272−1280.
(11) Zapf, A.; Beller, M. *Chem.—Eur. J.* **2001**, *7*, 2908−2915.
(12) Panin, A. N.; Dzhabieva, Z. M.; Nedorezova, P. M.; Tsvetkova, V. I.; Saratovskikh, S. L.; Babkina, O. N.; Bravaya, N. M. *J. Polym. Sci., Part A: Polym. Chem.* **2001**, *39*, 1915−1930.
(13) Cantrell, G. K.; Meyer, T. Y. *J. Am. Chem. Soc.* **1998**, *120*, 8035−8042.
(14) Babich, J. W.; Graham, W.; Femia, F. J.; Dong, Q.; Barzana, M.; Ferrill, K.; Fischman, A. J.; Zubieta, J. *Inorg. Chim. Acta* **2001**, *323*, 23−36.
(15) Papadopoulos, M.; Tsoukalas, C.; Pirmettis, I.; Nock, B.; Maina, T.; Abedin, Z.; Raptopoulou, C. P.; Terzis, A.; Chiotellis, E. *Inorg. Chim. Acta* **1999**, *285*, 97−106.
(16) Heimbold, I.; Drews, A.; Kretzschmar, M.; Varnas, K.; Hall, H.; Halldin, C.; Syhre, R.; Kraus, W.; Pietzsch, H. J.; Seifert, S.; Brust, P.; Johannsen, B. *Nucl. Med. Biol.* **2002**, *29*, 375−387.
(17) Mevellec, F.; Roucoux, A.; Noiret, N.; Patin, H. *Inorg. Chim. Acta* **2002**, *332*, 30−36.
(18) Nock, B.; Maina, T.; Tisato, F.; Papadopoulos, M.; Raptopoulou, C. P.; Terzis, A.; Chiotellis, E. *Inorg. Chem.* **2000**, *39*, 2178−2184.
(19) Mevellec, F.; Roucoux, A.; Noiret, N.; Patin, H. *J. Chem. Soc., Dalton Trans.* **2001**, 3603−3610.
(20) Nock, B.; Pietzsch, H. J.; Tisato, F.; Maina, T.; Leibnitz, P.; Spies, H.; Chiotellis, E. *Inorg. Chim. Acta* **2000**, *304*, 26−32.
(21) Herrmann, W. A.; Kratzer, R. M.; Fischer, R. W. *Angew. Chem., Int. Ed. Engl.* **1997**, *36*, 2652−2654.

10.1021/ic026174u CCC: $25.00

Chart 1

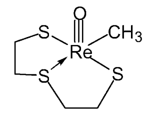

MeReO(SSS) **1**

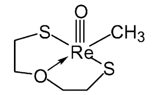

MeReO(SOS) **2**

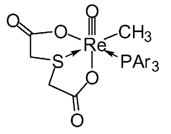

MeReO(OSO)PAr$_3$ **3**

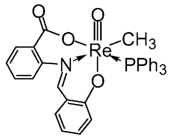

MeReO(ONO)PPh$_3$ **4**

methyl-oxorhenium(V) dimer, {MeReO(bt)$_2$}$_2$, was synthesized from MTO and benzenethiol, btH.[22] The tridentate ligand, 2-(salicylideneamino)benzoic acid (abbreviated HONOH) was synthesized from salicylaldehyde and 2-aminobenzoic acid.[23] Other ligands, the abbreviations of which follow from their chemical names: 2-mercaptoethyl sulfide (HSSSH), 2-mercaptoethyl ether (HSOSH), thioldiglycolic acid (HOSOH), and chemicals were purchased from Aldrich and used as received. Benzene-d_6 and chloroform-d_1 were employed as solvents for NMR spectroscopy. ACS grade chloroform was used as the solvent for UV−visible measurements.

A Bruker DRX-400 spectrometer was used to record the ^{1}H, ^{13}C, and ^{31}P spectra. The chemical shift for ^{1}H was defined relative to that of the residual proton of the solvent, δ 7.16 for benzene and δ 7.27 for chloroform. Shimadzu UV 3101PC and 2502PC spectrophotometers were used to record UV−visible spectra and monitor the reaction kinetics. Infrared spectra were determined with a Nicolet-500 spectrometer. Elemental analyses were performed by Desert Analytics Laboratory.

Syntheses of 1 and 2. These compounds were prepared from {MeReO(bt)$_2$}$_2$ (87 mg, 0.1 mmol) and the tridentate ligand (0.2 mmol) in 20 mL of toluene. After stirring the mixture for 4 h, 20 mL of hexanes was layered on the top of the solution and the mixture was placed in a freezer at ca. −12 °C. After 24 h a dark red powder had deposited; it was filtered and rinsed with hexanes. A crystal suitable for X-ray diffraction analysis was obtained by recrystallization from methylene chloride−hexanes. The acidic form of tridentate ligand can be abbreviated as HXYXH, thus the general chemical equation for these syntheses is

$$\{\mathrm{MeReO(bt)_2}\}_2 + 2\ \mathrm{HXYXH} \rightarrow 2\ \mathrm{MeReO(XYX)} + 4\ \mathrm{btH} \quad (1)$$

1 was obtained in 84% yield. NMR (Benzene-d_6) ^{1}H: δ 3.55 (s, 3H), 3.28 (m, 2H), 2.42 (m, 2H), 2.25 (m, 2H), 0.56 (m, 2H). ^{13}C: 48.0, 43.5, 5.1. IR (CHCl$_3$): 984 cm^{-1}. UV−Vis (CHCl$_3$), λ_{max}/nm (log ϵ/L mol^{-1} cm^{-1}): 252 (4.04) and 360 (sh). Elemental anal. $C_5H_{11}OReS_3$: found (calcd) C, 16.36 (16.25); H, 2.82 (3.00); S, 26.15 (26.03).

2 was obtained in 66% yield. NMR (Benzene-d_6) ^{1}H: δ 4.42 (s, 3H), 3.00 (m, 2H), 2.57 (m, 2H), 2.49 (m, 2H), 2.20 (m, 2H). ^{13}C: 85.1, 40.2, 4.0. IR (CHCl$_3$): 997 cm^{-1}. UV−Vis (CHCl$_3$), λ_{max}/nm: 290 (sh). Elemental anal. $C_5H_{11}O_2ReS_2$: found (calcd) C, 18.25 (16.99); H, 2.96 (3.14); S, 17.94 (18.14).

Syntheses of 3 and 4. These compounds were prepared from MTO (250 mg, 1 mmol), the tridentate ligand (1 mmol), and 2 mmol triphenylphosphane for **4** or the desired triarylphosphane for **3** in 20 mL of CH$_2$Cl$_2$. After stirring the mixture for 10 h, 20 mL of hexanes was layered on the top of the solution, and the mixture was placed in a freezer at ca. −12 °C. After 24 h a blue (**3**) powder or dark red (**4**) crystal had deposited. Each substance was filtered and rinsed by hexanes. The crystal of **4** directly from the synthesis was suitable for X-ray diffraction analysis. Recrystallization of **3** from methylene chloride−hexanes was needed to obtain diffraction-quality crystals. When the acidic form of the ligand is abbreviated HXYXH, the general chemical equation for the syntheses is

$$\mathrm{MeReO_3} + \mathrm{HXYXH} + \mathrm{PAr_3} \rightarrow \mathrm{MeReO(XYX)} + \mathrm{H_2O} + \mathrm{OPAr_3} \quad (2)$$

3−PPh$_3$ was obtained in 93% yield. NMR (chloroform-d_1) ^{1}H: δ 7.47∼7.70 (m, 15H), 4.58 (d, 3H), 3.61 (d, 1H), 3.36 (d, 1H), 2.89 (d, 1H), 1.38 (d, 1H). ^{13}C: 185.7, 177.8, 134.1 (d), 132.1 (d), 131.5 (d), 129.2 (d), 128.6 (d), 37.9, 36.6, 15.4. ^{31}P: 0.45. IR (CHCl$_3$): 1007 cm^{-1}. UV−Vis (CHCl$_3$), λ_{max}/nm: 265 (sh) and 300 (sh). Elemental anal. $C_{23}H_{22}O_5PReS$: found (calcd) C, 43.97 (44.01); H, 3.51 (3.53); S, 4.66 (5.11); P, 4.30 (4.93). **3**−OMe was synthesized from tris(4-methoxyphenyl)phosphane in 87% yield. NMR (chloroform-d_1) ^{1}H: δ 7.42∼7.47 (m, 6H), 7.00∼7.03 (m, 6H), 4.58 (d, 3H), 3.87 (s, 9H), 3.62 (d, 1H), 3.37 (d, 1H), 2.94 (d, 1H), 1.54 (d, 1H). ^{13}C: 185.8, 178.0, 135.6 (d), 134.0 (d), 123.0 (d), 114.7 (d), 114.2 (d), 55.5, 38.2, 36.7, 15.4. ^{31}P: −2.75. IR (CHCl$_3$): 1007 cm^{-1}. UV−Vis (CHCl$_3$), λ_{max}/nm: 350 (sh). **3**−F was synthesized from tris(4-fluorophenyl)phosphane in 88% yield. NMR (chloroform-d_1) ^{1}H: δ 7.50∼7.57 (m, 6H), 7.18∼7.28 (m, 6H), 4.51 (d, 3H), 3.64 (d, 1H), 3.43 (d, 1H), 3.02 (d, 1H), 1.63 (d, 1H). ^{13}C: 185.4, 177.9, 164.2 (q), 136.4 (q), 117.0 (m), 378.0, 36.4, 15.7. ^{31}P: δ −0.86. IR (CHCl$_3$): 1007 cm^{-1}. UV−Vis (CHCl$_3$), λ_{max}/nm: 300 (sh).

4 was obtained in 93% yield. NMR (Methylene chloride-d_2) ^{1}H: δ 8.01 (m, 1H), 7.65 (s, 1H), 7.57 (m, 1H), 7.48 (m, 1H), 7.29 (d, 1H), 7.03 (m, 1H), 6.78 (m, 2H), 6.56 (d, 1H) 4.40 (d, 3H). ^{13}C: too insoluble. ^{31}P: −7.18. IR (CHCl$_3$): 984 cm^{-1}. UV−Vis (CHCl$_3$), λ_{max}/nm: 300 (sh), 360 (sh) and 420 (sh). Elemental anal. $C_{33}H_{27}NO_4PRe$: found (calcd) C, 53.83 (55.15); H, 3.59 (3.79); N, 1.85 (1.95); P, 4.02 (4.31).

X-ray Structure Determination. The crystal evaluation and data collection were performed on a Bruker CCD-1000 diffractometer with Mo Kα (λ = 0.71073 Å) radiation, graphite monochromator, and a detector-to-crystal distance of 5.04 cm. All crystals were stable at ambient conditions, therefore routine procedures were used for mounting and centering of the samples. The data were collected by using the hemisphere (**1**, **2**) and full sphere (**3**, **4**) routines for better redundancy. Data sets were corrected for Lorentz and polarization effects. The multiscan absorption correction was based on fitting a function to the empirical transmission surface as sampled by multiple equivalent measurements using SADABS[24] software.

The positions of most of the atoms were found by direct (**1**, **2**) or Patterson (**3**, **4**) methods. The remaining non-hydrogen atoms were located in an alternating series of least-squares cycles on difference Fourier maps and were refined in full-matrix anisotropic approximation. All hydrogen atoms were placed in the structure factor calculation at idealized positions and were allowed to ride on the neighboring atoms with relative isotropic displacement coefficients. The calculations were performed with SHELXTL software package.[24]

Kinetics. Reactions of compound **2** with pyridine *N*-oxides were monitored by the decrease in absorbance of **2** at 525 nm. Concentrations of pyridine *N*-oxides were at least 10 times higher

---

(22) Takacs, J.; Cook, M. R.; Kiprof, P.; Kuchler, J. G.; Herrmann, W. A. *Organometallics* **1991**, *10*, 316−320.

(23) Westland, A. D.; Tarafder, M. T. H. *Inorg. Chem.* **1981**, *20*, 3992−3995.

(24) Blessing, R. H. *Acta Crystallogr., Sect. A* **1995**, *51*, 33−38.

Table 1. Crystallographic Data for Compounds **1**, **2**, **3**, and **4**

	1	**2**	**3**−PPh$_3$	**4**
color	dark red	dark red	blue	dark red
chemical formula	$C_5H_{11}OReS_3$	$C_5H_{11}O_2ReS_2$	$C_{23}H_{22}O_5PReS$	$C_{33}H_{27}NO_4PRe$
unit cell dimensions				
a, Å	8.9289(6)	7.8318(5)	21.682(8)	11.7111(15)
b, Å	8.9178(6)	10.4827(6)	10.833(4)	13.6521(16)
c, Å	11.8518(7)	10.9106(6)	19.248(7)	17.873(2)
β, deg	90	90.2451(10)	94.396(6)	100.867(2)
volume, Å	943.71(11)	895.73(9)	4508(3)	2806.3(6)
Z	4	4	8	4
formula wt	369.52	353.46	627.64	718.73
space group	*Cmc*2$_1$	*P*2$_1$/*n*	*C*2/*c*	*P*2$_1$/*n*
temp, K	173(2)	173(2)	173(2)	298(2)
wavelength, Å	0.71073	0.71073	0.71073	0.71073
density (calcd), Mg/m^3	2.601	2.621	1.850	1.701
abs coeff, mm^{-1}	13.476	13.974	5.587	4.427
R indices (all data)[a]	R1 = 0.0219 wR2 = 0.0573	R1 = 0.0325 wR2 = 0.0799	R1 = 0.0499 wR2 = 0.0881	R1 = 0.0349 wR2 = 0.0814
final R indices $[I > 2\sigma(I)]$[a]	R1 = 0.0215 wR2 = 0.0570	R1 = 0.0304 wR2 = 0.0788	R1 = 0.0408 wR2 = 0.0861	R1 = 0.0279 wR2 = 0.0757

[a] $R1 = \Sigma||F_0| - |F_c||/\Sigma|F_0|$; $wR2 = \{\Sigma[w(F_o^2 - F_c^2)^2]/\Sigma[w(F_0^2)^2]\}^{1/2}$.

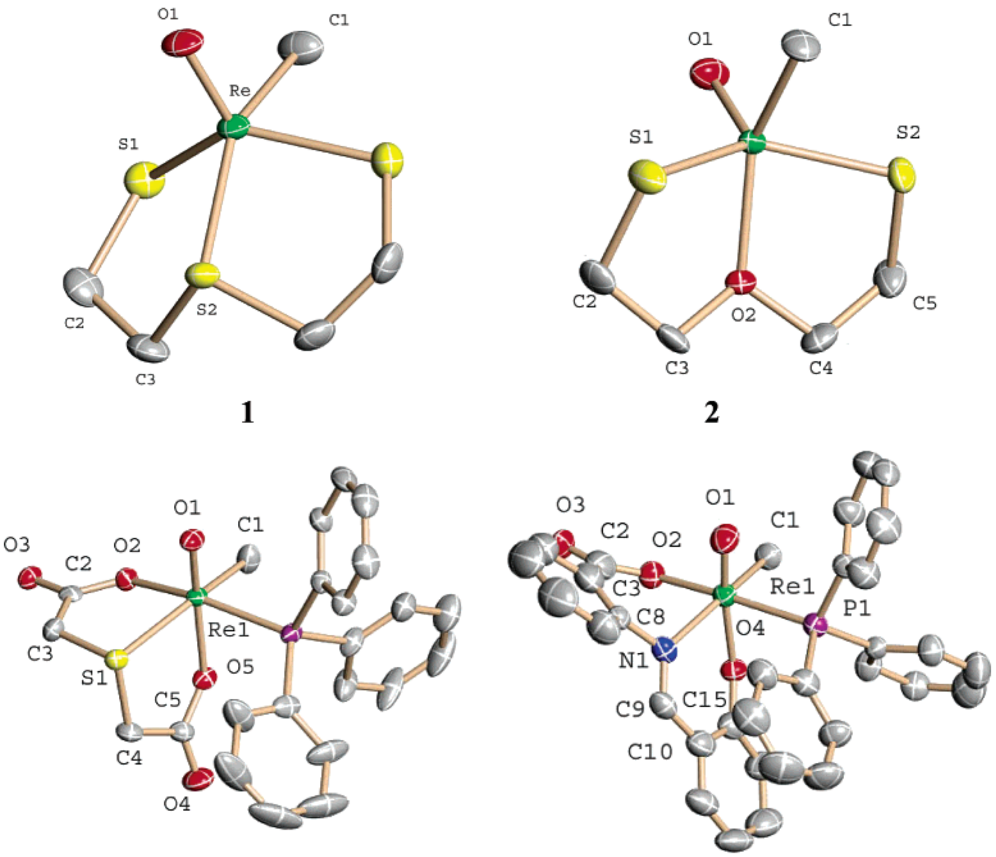

1

2

3

4

Figure 1. Crystallographically determined structures of **1**−**4**.

than that of **2**, allowing the absorbance-time data to be fitted to pseudo-first-order kinetics

$$\mathrm{Abs_t} = \mathrm{Abs_\infty} + (\mathrm{Abs_0} - \mathrm{Abs_\infty}) \times \exp(-k_\psi t) \qquad (3)$$

Reactions of compounds **3**−PPh$_3$, **3**−OMe, and **3**−F with pyridine *N*-oxides was carried out in the presence of the nucleophiles water, Cl$^-$, or methanol. Reactions were monitored by the changes in absorbance at 604, 367, and 350 nm according to the reagent used. The concentrations of the nucleophiles were at least 10-fold higher than that of **3**−L, allowing the absorbance-time data to be fitted to pseudo-first-order kinetics, according to eq 3. The stoichiometric reaction is

$$\mathrm{MeReO(OSO)(PAr_3) + 2PyO + H_2O \rightarrow MTO + Ar_3PO + HOSOH + 2Py} \qquad (4)$$

Results

Structures. Table 1 shows the crystallographic parameters for the four new oxorhenium(V) compounds and Figure 1 depicts their molecular structures.

Table 2 lists the important bond distances and angles of **1** and **2**. In both compounds, the rhenium atom lies at the center

Table 2. Selected Bond Lengths (pm) and Angles (°) of **1** and **2**

	1	**2**
Re−O(1)	168.9(4)	167.4(5)
Re−C(1)	216.3(6)	211.8(7)
Re−S(1)	228.46(10)	227.69(18)
Re−S(2) or Re−O(2)	233.86(19)	209.4(4)
Re−S(1a) or Re−S(2)	228.46(10)	227.55(17)

	1	**2**
O(1)−Re−C(1)	103.6(2)	101.3(3)
O(1)−Re−S(1)	115.45(4)	112.33(19)
O(1)−Re−S(2)	NA	112.00(19)
O(1)−Re−S(2) or O(1)−Re−O(2)	109.34(14)	116.1(2)
C(3)−S(2)−C(3a) or C(3)−O(2)−C(4)	101.9(3)	109.6(5)
C(3)−S(2)−Re or C(3)−O(2)−Re	108.02(4)	122.3(4)
S(1)−Re−S(1a) or S(1)−Re−S(2)	128.75(7)	135.67(7)
C(1)−Re−S(2) or C(1)−Re−O(2)	147.10(18)	142.6(2)

Table 3. Selected Bond Lengths (pm) and Angles (°) of **3** and **4**

	3	**4**
Re−O(1)	167.4(4)	168.1(3)
Re−C(1)	212.9(6)	213.8(4)
Re−P	244.69(15)	247.25(14)
Re−S or Re−N	253.37(16)	216.5(4)
Re−O(2)	203.3(4)	205.7(4)
Re−O(4)	203.9(4)	201.9(3)

	3	**4**
O(1)−Re−C(1)	103.1(2)	98.98(16)
O(1)−Re−S or N	93.92(15)	98.78(14)
O(1)−Re−P	92.18(14)	86.58(11)
O(1)−Re−O(2)	102.32(18)	98.38(13)
O(1)−Re−O(4)	165.76(18)	169.17(15)
C(3)−S−Re or C(8)−N−Re	95.66(19)	112.2(3)
C(4)−S−Re or C(9)−N−Re	100.5(2)	129.7(3)
C(3)−S−C(4) or C(8)−N−C(9)	103.0(3)	118.1(4)
P−Re−O(2)	164.43(11)	174.56(8)

of a distorted square-pyramid defined by its axial ligand, the terminal oxo group, and the equatorial plane occupied by the methyl group and three donor atoms of the tridentate ligand. The Re≡O distances are almost identical at 168 pm, and the Re−C bond distances are in the range 212−216 pm. The only difference between the two is that **1** has a thioether sulfur donor and **2** has an ether oxygen. It is notable that the C−O−Re angle is 122° around the ether oxygen atom of **2**, which is closer to 120° than the 108° C−S−Re angle around the thioether sulfur of **1**. It seems that the longer *d*(Re−S) of 234 pm, versus *d*(Re−O) 209 pm, allows greater flexibility in the five-membered rings of **1**.

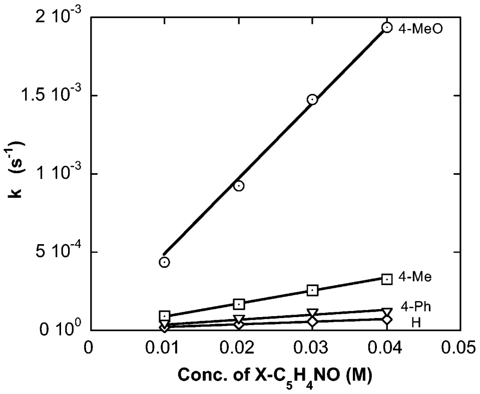

Figure 2. Plots of the pseudo-first-order rate constants for the reactions of **2** against the concentrations of pyridine *N*-oxides. The reaction was studied in $CHCl_3$ at 25 °C.

Table 3 summarizes the important bond distances and angles of **3** and **4**. In both compounds, the rhenium atom lies the center of a distorted octahedron defined by its axial ligands, the terminal oxo group, and one oxygen donor atom of the tridentate ligands, OSO and ONO. The Re≡O and Re−C distances are virtually identical in the two at 168 and 213 pm. The thioether Re−S distance in **3** is 19 pm longer than that in **1**, whereas the Re−N bond distance in **4**, 216 pm, lies in the normal range of Re−N single bonds, 211−220 pm.[25−27] The donor atoms trans to the terminal oxo groups in **3** and **4** do not lie notably closer or farther away from rhenium than do their counterparts in the equatorial plane. This is surprising because in other six-coordinate oxorhenium(V) compounds, the group trans to Re≡O lies at a longer distance.[25,28] Perhaps the structures of **3** and **4** reflect P−Re π back-bonding. In support of that we note that the ^{31}P chemical shifts of **3**−PPh_3 (δ 0.45) and **4** (−7.2)-lie near that of free PPh_3 (−4.4 ppm), whereas in other cases they are usually well downfield, MeReO(ethanedithiolate)-PPh_3 (δ −31.6 ppm) being typical.

Oxidation of 1. Compound **1** is the least reactive rhenium(V) compound that we have dealt with. For example, **1** is not oxidized by sulfoxides, pyridine *N*-oxides, or alkyl hydroperoxides. The decomposition of **1** with H_2O_2 is self-catalyzed owing to the generation of MTO, a well-known catalyst for the oxidation of organic or inorganic substrates by hydrogen peroxide.[29−32] The oxidation products are MTO and the cyclic disulfide, which were identified by NMR spectroscopy

$$1 + 2H_2O_2 \xrightarrow{\text{MTO}} \text{MTO} + S(CH_2CH_2S)_2 + 2H_2O \quad (5)$$

Oxidation of 2. Compound **2** is readily oxidized by sulfoxides and pyridine *N*-oxides to MTO and the cyclic disulfide

$$\text{MeReO(SOS)} + 2\text{PyO}/R_2SO \rightarrow \text{MTO} + O(CH_2CH_2S)_2 + 2\text{Py}/R_2S \quad (6)$$

Kinetic studies of the oxidation of **2** with pyridine *N*-oxides were carried out at 25 °C in chloroform. Figure 2 depicts the pseudo-first-order rate constants against the concentration of pyridine *N*-oxide and its aromatic ring-substituted derivatives. The data form straight lines that pass through

---

(25) Espenson, J. H.; Shan, X.; Lahti, D. W.; Rockey, T. M.; Saha, B.; Ellern, A. *Inorg. Chem.* **2001**, *40*, 6717−6724.

(26) Lente, G.; Guzei, I. A.; Espenson, J. H. *Inorg. Chem.* **2000**, *39*, 1311−1319.

(27) Lente, G.; Jacob, J.; Guzei, I. A.; Espenson, J. H. *Inorg. React. Mechs.* **2000**, *2*, 169−177.

(28) Shan, X.; Ellern, A.; Espenson, J. H. *Inorg. Chem.* **2002**, *41* (26), 7136−7142.

(29) Abu-Omar, M. M.; Espenson, J. H. *J. Am. Chem. Soc.* **1995**, *117*, 272−280.

(30) Al-Ajlouni, A. M.; Espenson, J. H. *J. Am. Chem. Soc.* **1995**, *117*, 9243−9250.

(31) Espenson, J. H. *Chem. Commun.* **1999**, 479−488.

(32) Espenson, J. H.; Abu-Omar, M. M. *Adv. Chem. Series* **1997**, *253*, 99−134.

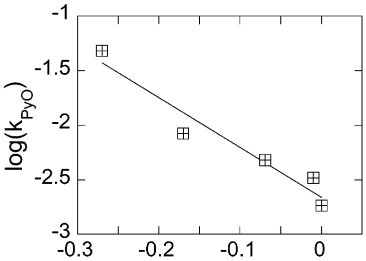

Figure 3. Analysis of the rate constants for the oxidation of **2** by pyridine *N*-oxide by the Hammett equation.

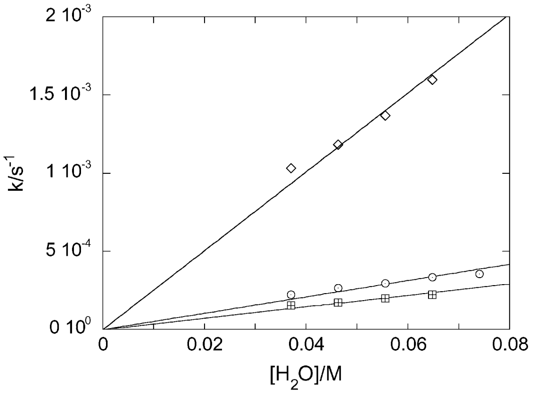

Figure 4. Plots of the pseudo-first-order rate constants for the reactions of the three derivatives of **3** against the concentration of water. The reaction was studied in $CHCl_3$ at 25.0 °C.

Table 4. Rate Constants for the Oxidation of **2** by Ring-Substituted Pyridine *N*-Oxides

$X-C_5H_4NO$	$k_{PyO}/10^{-3}$ L mol^{-1} s^{-1}
4-MeO	48.2(7)
4-Me	8.4(1)
3-Me	4.8(1)
4-Ph	3.3(2)
H	1.84(3)

the origin. Thus, the rate equation is

$$-\frac{d[\mathbf{2}]}{dt} = k[\mathbf{2}]\cdot[X - C_5H_4NO] \tag{7}$$

The second-order rate constants are listed in Table 4. 4-Methoxypyridine *N*-oxide, with the most electron-donating substituent, is the most reactive, with $k = (4.82 \pm 0.07) \times 10^{-2}$ L mol^{-1} s^{-1}. An analysis of the rate constants by the Hammett equation is presented in Figure 3; it gives a remarkably large and negative reaction constant, $\rho = -4.6$. This suggests a multistep reaction sequence.[9] The reaction rate was not changed by the deliberate addition of water or methanol.

Oxidation of 3. Compound **3**−PPh_3 and its PAr_3 ring-substituted derivatives are oxidized to MTO, phosphane oxide, and thioldiglycolic acid, as in eq 4, by pyridine *N*-oxides in chloroform in the presence of water.

These reactions show first-order dependences on [H_2O] and [**3**]. Figure 4 depicts the pseudo-first-order rate constants for the three derivatives of **3** against the concentration of water, and the second-order rate constants are listed in Table 5.

Varying the concentration of 4-picoline *N*-oxide from 20 mM to 40 mM gave the same rate constant, $(3.9 \pm 0.1) \times 10^{-3}$ (20 mM 4-PicO) and $(4.0 \pm 0.1) \times 10^{-3}$ L mol^{-1} s^{-1} (40 mM 4-PicO). Different pyridine *N*-oxides also gave the same value of rate constant: $(3.9 \pm 0.1) \times 10^{-3}$ (20 mM 4-PicO) and $(4.0 \pm 0.1) \times 10^{-3}$ L mol^{-1} s^{-1} (20 mM 4-Ph-C_5H_4NO).

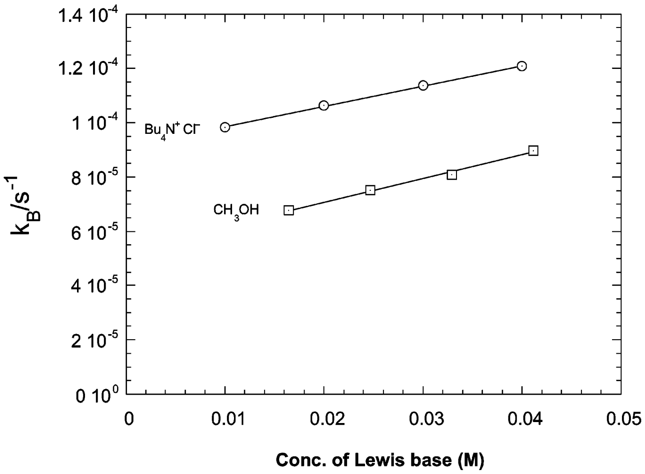

Figure 5. Effect of other nucleophiles, Cl$^-$ and MeOH, on the oxidation of **3** is proportional to [Nu] in $CHCl_3$ at 25 °C. The intercepts reflect the effect of the residual water in the solutions.

Table 5. Rate Constants for the Oxidation of **3** and Its Derivatives with Ring-Substituted Triphenylphosphanes by 4-Picoline *N*-Oxide at Presence of Nucleophiles

reactant	Lewis base	$k/10^{-3}$ L mol^{-1} s^{-1}
3−PPh_3	H_2O	3.9(1)
3−PPh_3	D_2O	3.6(2)
3−PPh_3	CH_3OH	0.88(5)
3−PPh_3	$Bu_4N^+Cl^-$	0.75(1)
3−OMe	H_2O	2.59(9)
3−F	H_2O	20(1)

The substituents on the aromatic ring of PAr_3 coordinated to rhenium in compound **3** show considerable effect. Second-order rate constant of **3**−F, with the most electron withdrawing substituent, is almost 10-fold bigger than that of **3**−OMe, containing the most electron-donating substituent.

Deuterated water was employed to check for a kinetic isotope effect. It gave the same value of rate constant: $(3.9 \pm 0.1) \times 10^{-3}$ (H_2O) and $(3.6 \pm 0.2) \times 10^{-3}$ L mol^{-1} s^{-1} (D_2O). Also other nucleophiles, Cl$^-$ and methanol, were found to accelerate the oxidation of **3** with 4-picoline *N*-oxides. The reactions show first-order dependences on the concentrations of the nucleophile and **3**. Figure 5 depicts the pseudo-first-order rate constants against the concentration of nucleophiles; the rate constants are listed in Table 5.

Discussion

Mechanism of the Oxidation of 2. Scheme 1 shows the proposed mechanism for oxidation of **2**. No doubt, coordination of pyridine *N*-oxides to rhenium is the first step of oxidation of **2**, as there is an empty position trans to the terminal oxo group.

The reaction begins with the coordination of PyO at the vacant coordination site on **2**. This particular reaction cannot be evaluated because of the subsequent reactions that ensue. But with different ligands that do not react further, some definite statements can be made. With monodentate ligands, even those that might be anticipated to have large values of

Scheme 1. Direct Oxidation of 2 by Pyridine N−Oxide

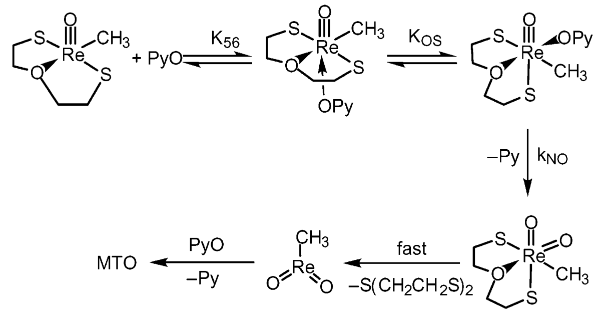

Scheme 2. Nucleophile-Induced Pathway for the Oxidation of 3 by PyO

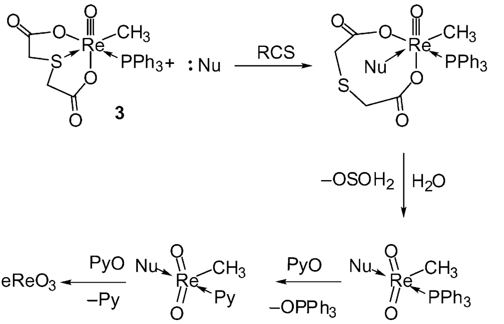

K_{56}, a six-coordinate complex never builds up to a detectable level. Only with a bidentate ligand such as 2,2′-bipyridine, where the chelate effect dominates, does a six-coordinate species form to a measurable extent. On that basis, it appears that the equilibrium constant in Scheme 1 is $K_{56} \ll 1$. In other words, the enthalpy gain from the formation of a Re−O bond is minimal. According to our earlier work, the PyO enters the equatorial plane by way of a turnstile rotation mechanism.[33] The driving force for the isomerization is to avoid, after the Py−O bond cleavage, formation of a *trans*-dioxorhenium(VII) intermediate, which would lie at a much higher energy for a d^0 species than would the cis isomer.[34,35] Unlike previous work on oxidation of rhenium compounds containing a dithiolate ligand,[9] all of the intermediates are six-coordinate without further addition of another molecule of pyridine *N*-oxide because of the chelating tridentate ligands.

Because a thiolate sulfur is more strongly bound to rhenium than an oxygen atom donor, $K_{OS} \ll 1$. Clearly the cleavage of the N−O bond is the rate-controlling step. The dramatic electronic effect of the substituents on the pyridine *N*-oxides comes from the combined term represented by the experimental $k = K_{56}K_{OS}k_{NO}$. Each of the three components of k can be expected on the basis of the chemistry at that step to contribute a negative value to the overall value of the reaction constant: $\sigma_k = \sigma_{56} + \sigma_{OS} + \sigma_{NO}$. The steps following the rate-controlling step were proposed without further experimental evidence explicit to this case; they are, however, consistent with the known chemistry of these compounds which, at the Re(VII) stage, oxidize dithiolates to disulfides.[1,36]

Scheme 1 is also suitable for the oxidation of **1**, and its lower reactivity with pyridine *N*-oxides must come from smaller values of K_{OS} and k_{NO} caused by the trans effect from thioether sulfur, a better electron donor than the ether oxygen of **2**.

Mechanism of the Oxidation of 3. The kinetics of oxidation of **3** shows first-order dependences on [**3**] and [H_2O], but the rate is independent of [PyO]. Pyridine *N*-oxide is, however, required to complete the stoichiometric transformation. Once the involvement of water was suspected, this was checked by its deliberate addition at known levels. Because there is no H−D kinetic isotope effect, it is not likely that H_2O or D_2O attacks directly at a carboxylato oxygen. We propose that attack is instead at rhenium, accompanying which the Re−S bond to the thioether is broken. Formation of an initial Re−OH_2 bond not only assists in ligand hydrolysis, but also advances the formation of one of the new Re═O bonds that must appear in the product. The rate constants for H_2O attack lie in the order **3**−F > **3**−PPh_3 > **3**−OMe, as one would expect for a mechanism involving initial nucleophilic attack at rhenium.

This formulation suggests that nucleophiles other than H_2O should be able to carry out the first, non-hydrolytic step. That indeed proved so, and both Cl^- and MeOH reacted in a catalytic fashion and were not transformed during the reaction. The rate law in these cases was k[**3**][Nu]. With these nucleophiles as well, the rate is not dependent on [PyO].

Scheme 2 shows the sequence of proposed reactions. Because the rates are independent of [H_2O], it must enter later, and so it is reasonable to interpret the data in terms of nucleophilic attack as being rate-controlling.

Steric Influences. The different pathways adopted for the oxidation of **2** and **3** can be traced to their different coordination numbers, which creates a higher steric demand for **3**. This can be seen from second-order rate constants (L mol^{-1} s^{-1}) of oxidation of **3** with presence of different nucleophiles: $(3.9 \pm 0.1) \times 10^{-3}$ (H_2O), $(0.88 \pm 0.05) \times 10^{-3}$ (MeOH), and $(0.75 \pm 0.01) \times 10^{-3}$ (Cl^-). Both MeOH and Cl^- are stronger nucleophiles than water, but the reaction with water is 4−5 times faster. The steric demands of MeOH (195 pm van der Waals radius)[37] and Cl^- (180 pm ionic radius) exceed that of water (140 pm van der Waals radius).[38]

Acknowledgment. This research was supported by the U. S. Department of Energy, Office of Basic Energy Sciences, Division of Chemical Sciences under contract W-7405-Eng-82.

Supporting Information Available: Plots of kinetic data and complete tables of crystal data and refinement details, atomic coordinates, bond lengths and angles, and anisotropic displacement parameters (24 pages; pdf). This material is available free of charge via the Internet at http://pubs.acs.org.

IC026174U

---

(33) Lahti, D. W.; Espenson, J. H. *J. Am. Chem. Soc.* **2001**, *123*, 6014−6024.

(34) Barea, G.; Lledos, A.; Maseras, F.; Jean, Y. *Inorg. Chem.* **1998**, *37*, 3321−3325.

(35) Mingos, D. M. P. *J. Organomet. Chem.* **1979**, *179*, C29−C33.

(36) Jacob, J.; Guzei, I. A.; Espenson, J. H. *Inorg. Chem.* **1999**, *38*, 3266−3267.

(37) Khimenko, M. T. *Zh. Fiz. Khim.* **1969**, *43*, 1861−1864.

(38) Goede, A.; Preissner, R.; Froemmel, C. *J. Comput. Chem.* **1997**, *18*, 1113−1123.